UDC669.14.018.85:662.922.2

New Corrosion-Resistant Steel Plate (WELACC5) for LNG Funnel

Akira Usami*1
Takeshi Tsuzuki*3
Hidesato Mabuchi*1
Ryuichiro Ebara*4
Kouji Tanabe*2
Tadashi Kasuya*1
Yukio Tomita*1
Hiroshi Kondo*4

Abstract:

A new corrosion-resistant plate steel, designated WELACC5 (well anti-corrosion steel containing Cr 5% with weldability for advanced combined cycle), was developed. WELACC5 can be used unpainted and free from maintenance in the stack environment of LNG-fired power plants for long periods of time. The corrosion rate of WELACC5 in the LNG-fired power plant stack environment is 0.0007 mm/y and is far smaller than that of carbon steel. A tight and difficult-to-scatter rust film is formed on the surface of WELACC5 in the stack environment. The mechanical properties, formability, weldability, and weld joint performance of WELACC5 are equivalent to those of carbon steel. The satisfactory performance of WELACC5 as stack plate steel was verified by evaluating mill trial plates. As of 1997, more than 2,000 tons of WELACC5 was produced for the stacks of LNG-fired combined cycle power plants.

1. Introduction

In recent years, against a backdrop of global environmental problems and fuel diversification measures, many thermal power plants fueled by liquefied natural gas (LNG) or liquefied petroleum gas (LPG) have been constructed, mainly in urban areas, in addition to conventional oil- and coal-fired thermal power plants.

Generally, the steel stacks of thermal power plants are lined with castable and other inorganic materials to protect their steel shell. Many of the stack linings deteriorate with age under the influence of corrosive components and heat of the flue gas, so that shell damage and lining dislodgment become problems for some stacks. The repair period sometimes necessitates plant shutdown, incurring great loss[1]. For this reason, recent stack shells have increasingly been made of steels with higher corrosion resistance for maintenance-free operation.

Nippon Steel developed and commercialized such a maintenance-free steel, a sulfuric acid dew-point corrosion-resistant stainless steel, called YUS260[2]. Sulfuric acid dew-point corrosion-resist-

*1 Steel Research Laboratories
*2 Nippon Steel Techno Research Corporation
*3 Nagoya Works
*4 Mitsubishi Heavy Industries, Ltd.

ant low-alloy steels, represented by Nippon Steel's S-TEN steel, also have many service results[3]. Each of these metallic materials was developed for use in the flue gas environment of power plants burning fossil fuels such as oil or coal.

The stacks of LNG-fired plants have pressing needs to lower their construction and maintenance costs. New corrosion-resistant steels capable of assuring economical and maintenance-free operation were in strong demand. Nippon Steel thought that the requirements for superior economy and maintenance-free operation could be met by the development of a low-alloy steel that corrodes at a low rate and forms a tightly adherent rust film in the LNG-fired plant stack environment. Based on this thinking, Nippon Steel developed a new corrosion-resistant plate steel (trademarked WELACC5) for LNG-fired power plant stacks in cooperation with Mitsubishi Heavy Industries. WELACC5 allows these stacks to be operated free of maintenance without castable linings for a long period of time and is more economical than stainless-clad carbon steel in this application.

This article reports the development history of WELACC5 and its service performance properties.

2. Development History of WELACC5

The flow of development was as follows. First, the corrosive environment of stacks was investigated, and simulative corrosion test methods were developed according to the results of investigation. The effects of alloying elements on the corrosion resistance and rust adhesion of stack steels were clarified by simulative corrosion tests. The optimum basis composition system was derived, and its performance was verified in exposure tests at an LNG-fired power plant. The new steel was trial produced at the mill and investigated for its manufacturability and fabricability.

2.1 LNG-fired power plant stack environment and alloy design considerations

2.1.1 Corrosion environment of LNG-fired power plant stack

The temperature of LNG-fired combined cycle power plant flue gas at the stack inlet is 373 to 383K during normal operation and about 408K during abnormal operation. The flue gas is said to be typically composed of 6 to 10 vol% H_2O, 3 vol% CO_2, 14 vol% O_2, and 73 to 77 vol% N_2. When the inside surface temperature of the stack shell in contact with the flue gas drops below the dew point of sulfuric acid at oil- and coal-fired power plants, sulfuric acid condenses to a high concentration and causes sulfuric acid dew-point corrosion. At an LNG-fired power plant, sulfuric acid condensation does not take place because the fuel or LNG contains no sulfur. Instead, corrosion due to the condensation of water vapors in the flue gas, or what is called water corrosion, occurs. When the plant is daily started and stopped, the temperature of the stack inside surface falls below the dew point of water, and condensed water forms on the inside surface of the stack. The resultant aqueous solution that contains the flue gas and ash, among other things, is considered to cause alternate wet and dry corrosion eventually.

Table 1 lists the chemical analysis results of water-soluble ions present in deposits on the inside surface of an LNG-fired power plant stack and of the drain from the stack. Both deposits and drain are mainly composed of sulfate ions and were weakly acidic with a pH of 3.6 to 4.4. NH_4^+ and Cl^- were also recognized. NH_4^+ was probably a carryover from a flue gas denitrification system. Cl^- was detected probably due to ultratrace constituents in the flue gas or sea salt particles in the air, but details are unknown. Among other probable corrosive factors are sulfur compounds (mercaptans) in the fuel, and formaldehyde, formic acid and nitrogen dioxide (NO_2) formed during incomplete combustion. These substances were not detected in the corrosion survey of the stack.

Fig. 1 shows the relationship between typical steel service environments and LNG-fired power plant stack environments. The corrosive environment of the LNG-fired power plant stack is created by the weakly acidic condensed water in which are dissolved flue gas components and deposits, and is relatively close to an atmospheric corrosion environment among general corrosive environments.

2.1.2 Alloy design considerations

From the corrosive environment survey results, it was predicted that alternate wetting and drying corrosion by the aqueous solution in which carbon dioxide (CO_2) from the flue gas is dissolved would be predominant in the LNG-fired power plant stack environment. Chromium, which is known to improve CO_2 corrosion resistance, was selected as the first alloying element to be added. The chromium content was set at 3 to 9%, so that the final form of corrosion would be general corrosion, not local corrosion. From the standpoint of rust scatter resistance, copper, nickel, and molybdenum were added in the expectation that they would improve rust adhesion.

The chemical compositions of low-alloy steels trial produced according to the above considerations are given in **Table 2**. Each prototype steel was vacuum melted in an amount of 50 kg, hot rolled to 6- and 12-mm thick plates, heat treated if necessary, and used to take various specimens. The commercially available SM400, SUS304, and SUS316 steels were employed as control materials.

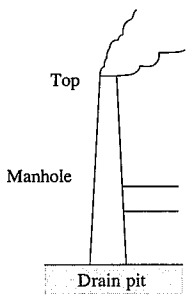

Table 1 Water-soluble ions in deposits on inside surface of LNG-fired power plant stack (mass%)

	Top		Manhole			Drain pit	
	T1	T2	M1	M2	M3	DH	DP
	Precipitate	Precipitate	Precipitate	Precipitate	Rust	Aqueous solution	Aqueous solution
pH	4.4	4.1	6.4	7.3	3.8	4.0	3.6
Fe^{3+}	0.01	-	-	-	-	-	-
Fe^{2+}	0.06	0.02	-	-	-	-	-
NH_4^+	7.50	0.38	0.15	-	0.28	102ppm	92ppm
Cl^-	<0.02	0.08	0.29	0.14	0.19	19ppm	19ppm
SO_4^{2-}	26.0	5.70	23.0	7.20	1.82	360ppm	350ppm

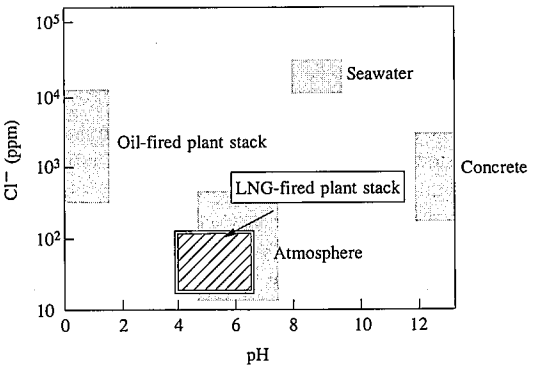

Fig. 1 Corrosive environment of LNG-fired power plant stack

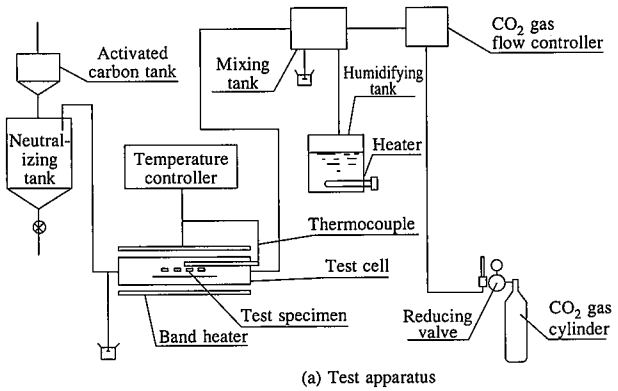

(a) Test apparatus

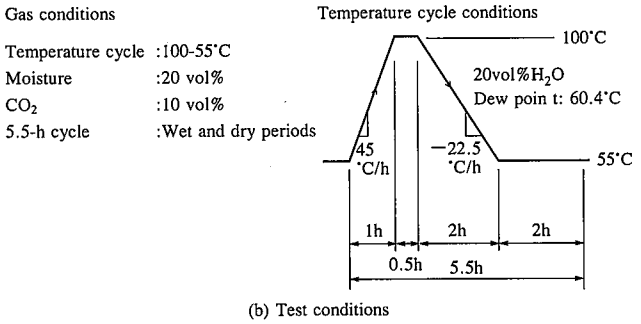

(b) Test conditions

Fig. 2 Alternately wet and dry CO_2 gas corrosion test

Table 2 Chemical compositions of test steels (mass%)

Steel	C	Si	Mn	P	S	Cu	Ni	Cr	Mo
3Cr	0.030	0.21	0.48	0.006	0.001	-	-	3.03	-
5Cr	0.032	0.19	0.50	0.001	0.001	-	-	5.04	-
7Cr	0.030	0.20	0.49	0.005	0.001	-	-	6.97	-
9Cr	0.028	0.21	0.49	0.005	0.001	-	-	8.56	-
3Cr-0.5Mo	0.030	0.20	0.49	0.001	0.001	-	-	2.99	0.52
5Cr-0.5Mo	0.030	0.20	0.50	0.005	0.001	-	-	5.11	0.52
5Cr-1.5Ni	0.030	0.20	0.49	0.001	0.001	-	1.48	4.93	-
5Cr-0.3Cu-0.3Ni	0.029	0.20	0.51	0.001	0.001	0.34	0.30	5.02	-
SM 400B	0.120	0.19	0.85	0.013	0.009	0.01	0.02	-	-
SUS 304	0.060	0.48	0.86	0.028	0.007	-	8.65	18.26	-
SUS 316L	0.020	0.48	0.85	0.026	0.001	-	12.21	17.35	2.18

2.2 Effect of alloy composition on corrosion resistance

2.2.1 Corrosion test method considerations

When studying corrosion resistance, the corrosion process of the LNG-fired power plant stack was divided into two parts (a) and (b) during start and stop and during normal operation, respectively. The process (a) is that of alternate wetting and drying corrosion caused by boiler start and stop. The process (b) is that of corrosion caused by a small amount of moisture present between the deposits and the steel surface when the temperature is relatively low due to boiler operating conditions. For the process (a), alternately wet and dry CO_2 gas corrosion test was conducted to evaluate corrosion resistance in a simulative gas environment, and intermittent immersion corrosion test was conducted to evaluate corrosion resistance under the influence of a simulative aqueous solution. For the process (b), immersion corrosion test was conducted in simulative deposited ash.

2.2.2 Corrosion test methods

(1) Alternately wet and dry CO_2 gas corrosion test

Using the apparatus shown in **Fig. 2**, the alternately wet and dry CO_2 gas corrosion test was conducted for a maximum of about 181 cycles (1,000 h), each cycle (5.5 h) consisting of heating, holding, and cooling periods in the temperature range of 328 to 373K by considering the operating conditions of the actual stack[3].

(2) Intermittent immersion corrosion test

Specimens are immersed in a simulative aqueous solution adjusted to a desired composition based on the analytical results of deposited ash and drain, are removed from the aqueous solution, and are dried. The simulative aqueous solution was prepared by dissolving $(NH_4)_2SO_4$, Na_2SO_4 and NaCl to 440, 140 and 40 ppm, respectively, in distilled water and adjusting with diluted sulfuric acid to a pH of 4.0. One cycle consisted a 2-min immersion period and a 58-min drying period (for total of 1 h). The test was conducted for a maximum duration of 236 h (236 cycles).

(3) Simulative deposited ash immersion corrosion test

Plate specimens were completely buried in the simulative deposited ash composed of 0.8 g $(NH_4)_2SO_4$, 0.2 g Na_2SO_4, 0.02 g NaCl and 40 mass% water, and were held for 1 month in a cabinet maintained at a constant temperature of 353K and a constant relative humidity of 70%. When the weight of the cell was periodically measured during the test, it exhibited no large weight change with water vaporization and condensation. The moisture content of the simulative deposited ash is thus considered to have remained almost constant during the test duration.

2.2.3 Effect of alloy composition on corrosion resistance

(1) Effect of chromium addition on corrosion resistance

Fig. 3 shows the effect of chromium addition on the corrosion rate of steels in the alternately wet and dry CO_2 gas corrosion test. From these results, it is clear that the chromium addition is extremely effective in improving corrosion resistance. The addition of 5% chromium is found to effectively provide desired corrosion resistance. The SUS304 and SUS316L steels exhibited little corrosion weight loss under any test conditions. The intermittent immersion corrosion test and simulative deposited ash immersion corrosion test produced the results that the addition of 5% chromium also improved the corrosion resistance of the test steels.

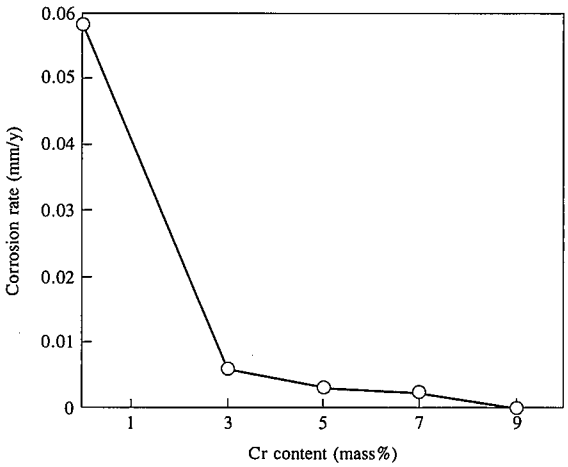

Fig. 3 Effect of chromium content on corrosion rate (after 248 h of alternately wet and dry CO_2 gas corrosion test)

(2) Effects of copper, nickel, and molybdenum additions on corrosion resistance of 5Cr steel

Fig. 4 compares the corrosion rate of the test steels in the alternately wet and dry CO_2 gas corrosion test. The corrosion rate of the 5Cr steel was reduced by about 20% when copper and nickel were added in combination and when nickel and molybdenum were added singly. In the intermittent immersion corrosion test and simulative deposited ash immersion corrosion test, the copper, nickel, and molybdenum additions did not significantly reduce the corrosion rate of the 5Cr steel. The corrosion rate of the 5Cr steel to which were added copper, nickel, and molybdenum was almost equal to that of the 5Cr steel without such additions.

The above results indicate that the combined addition of copper and nickel and the single addition of nickel and molybdenum to the 5Cr steel improve the corrosion resistance of the 5Cr steel, depending on corrosion conditions, and do not detract from the corrosion resistance of the 5Cr steel.

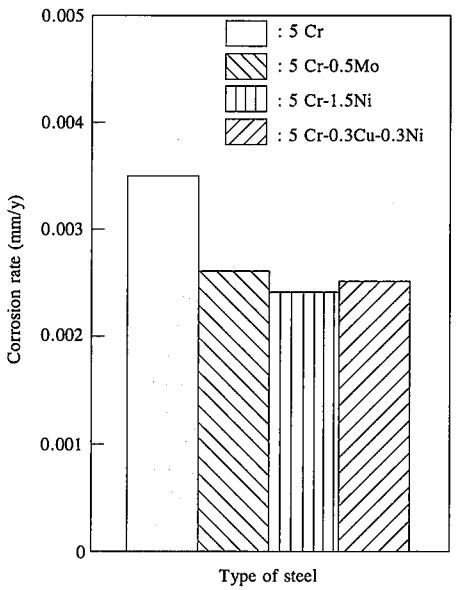

Fig. 4 Effects of alloying elements on corrosion rate of 5Cr steel (after 1,000 h of alternately wet and dry CO_2 gas corrosion test)

2.2.4 Anodic and cathodic polarization behavior in stack environment

To study the effects of the chromium addition and the copper-nickel, nickel and molybdenum additions to the 5Cr steel in inhibiting the corrosion rate as revealed by the corrosion tests described above and the effect of the flue gas on the corrosion reactions, a simulative aqueous solution of the same composition as used in the intermittent immersion corrosion test was sparged with a gas mixture (CO_2:O_2:N_2 = 11:1.5:balance) simulating the flue gas, air and argon, and cathodic polarization behavior was investigated by the potential scanning method in the simulative aqueous solution deaerated with argon.

Fig. 5 shows the anodic polarization curves of the test steels. Since the anodic polarization increases with increasing chromium content, chromium is considered to control the anodic reactions. When the copper-nickel, nickel, and molybdenum additions were similarly investigated for their effects on the anodic polarization behavior of the 5Cr steel, they slightly increased the anodic polarization, but those increases were not as clear as those observed with the chromium.

Fig. 6 shows the cathodic polarization curves of the 5Cr steel under different sparging conditions. Sparging with the flue gas is

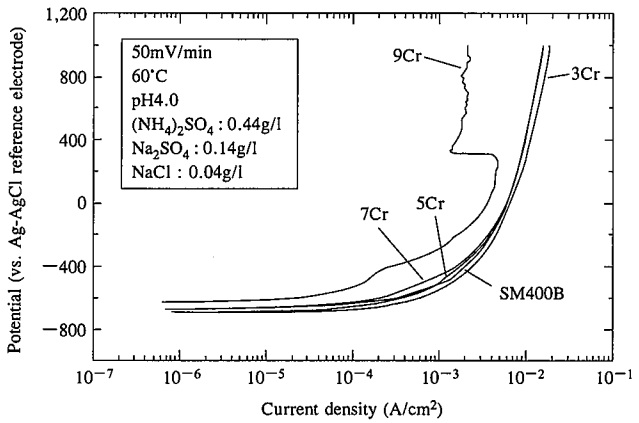

Fig. 5 Effect of chromium content on anodic polarization behavior

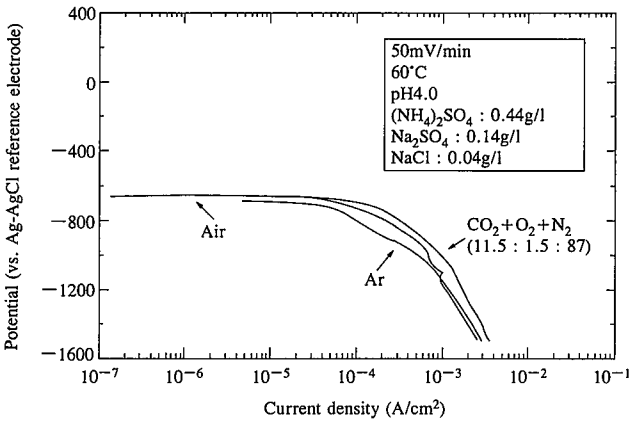

Fig. 6 Effect of sparge gas on cathodic polarization behavior of 5Cr steel

found to accelerate the cathodic reactions as compared with the case in which the aqueous solution was deaerated with argon or was open to the atmosphere. This may be attributed to the buffer action of CO_2 dissolved in the aqueous solution. The phenomenon that the cathodic reactions are accelerated by sparging with the flue gas was also recognized in the cathodic polarization behavior when the saturated solution of compound salts used in the simulative deposited ash immersion corrosion test was sparged with the simulative gas.

From these results, it is presumed that CO_2 in the flue gas accelerates the cathodic reactions in the LNG-fired power plant stack environment and that the corrosion rate of the chromium-bearing steels is lowered because the chromium inhibits the anodic reactions.

2.3 Effect of alloy composition on rust stability

When the stack shell is made of an unpainted low-alloy steel, a relatively tight corrosion product (rust) film is predicted to cover the steel surface during service. In this case, the corrosion product should

1) be small in the amount of formation,
2) have good adhesion, and
3) be uniformly formed on the steel surface.

The trial steels were investigated for rust properties, and the effect of alloy composition on rust stability was studied. Specimens after 236 cycles of the intermittent immersion corrosion test were evaluated for the amount of rust formation by measuring the weight of deposited rust, for the formation of relatively easy-to-peel rust by observing the rusted steel surface under a stereomicroscope, for the uniformity of rust film formation by observing the rust film/steel base interface, and for the tightness of rust film constituent particles by observing the rust particles under a transmission electron microscope (TEM). Their rust film/steel base interface was also analyzed for elements by an electron-probe microanalyzer (EPMA).

Fig. 7 shows the effect of chromium content on the rust amount (sum of the weight of peeled rust and the weight of adherent rust). The total rust weight is governed by the chromium content and is correlated well with the corrosion weight loss.

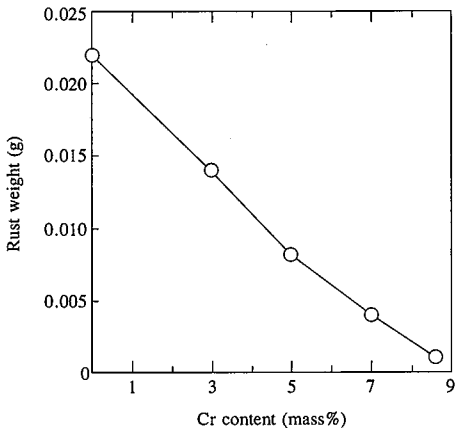

Fig. 7 Effect of chromium content on rust weight (after 236 h of intermittent immersion corrosion test)

Stereomicroscopy found that the SM400B steel was covered by coarse, granular, and peelable loose rust and that the formation of granular and peelable loose rust is inhibited as the chromium content increases. The 5Cr steel specimens to which were added copper, nickel, and molybdenum in various amounts had a smaller formation of granular and peelable loose rust than the 5Cr steel specimens without such copper, nickel, and molybdenum additions.

Fig. 8 shows the rust adhesion evaluation results of the SM400B, 5Cr, and 5Cr-0.3Cu-0.3Ni steels. The adhesion of rust was evaluated by the tape peel test. An adhesive tap was applied to a rusted specimen surface and then rapidly removed from the rusted specimen surface with a swift, jerking motion. The rust adhered to the tape was defined as "peeled rust", and the rust left attached to the specimen surface was defined as "adherent rust". The rust adhesion of the test specimen was evaluated by weighing these two types of rust. When the 5Cr steel and the 5Cr-0.3Cu-0.3Ni steel were compared, they were approximately the same in the amount of rust formation, but the 5Cr-0.3Cu-0.3Ni steel increased in the proportion of the adherent rust and decreased in the proportion of the peeled rust. The improved rust adhesion recognized with the 5Cr-0.3Cu-0.3Ni steel was also recognized with the 5Cr-1.5Ni and 5Cr-0.5Mo steels.

Optical micrographs of the steel base/rust film interfaces are presented in **Photo 1**. In the SM400 steel, the rust film thickness was nonuniform and exceeded 100 μm in localized portions, and granular and peelable loose rust was recognized as is evident in the micrograph. The rust film thickness was small and uniform, and ranged from 10 to 30 μm in the steels containing 3% or more chromium. The 5Cr steels to which were added copper, nickel, and molybdenum separately had more uniform rust film thickness than the 5Cr steel. The formation of a tightly adherent rust film was confirmed.

The TEM observation of rust particles found that the formed rust consisted of colloidal aggregations of iron oxide hydroxide and of coarse needlelike and crystallized particles and fine primary particles. These results were similar to those of particles comprising the rust film formed on low-alloy steels exposed to the atmosphere[4]. There were many coarse, needlelike particles, measuring 1 μm or more in size, for the SM400B steel, but the number of such coarse particles was smaller for the 5Cr steel. **Photo 2** shows typical TEM micrographs of rust particles on the 5Cr steel and 5Cr-0.3Cu-0.3Ni steel. The 5Cr-0.3Cu-0.3Ni steel had the formation of

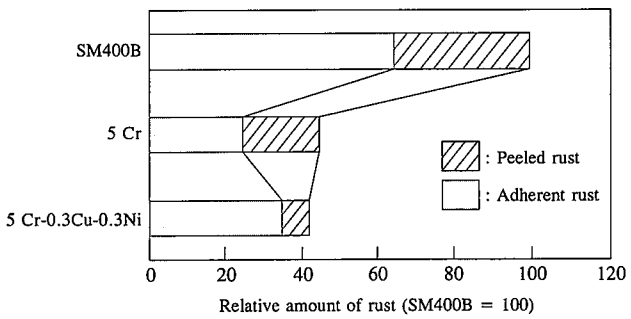

Fig. 8 Effect of alloying elements on rust weight (after 236 h of intermittent immersion corrosion test)

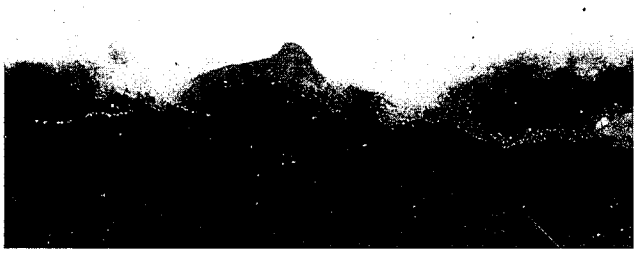

(a) SM400B

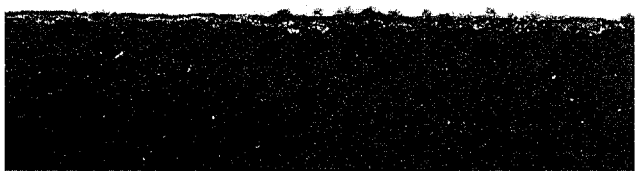

(b) 5Cr-0.3Cu-0.3Ni

Photo 1 Rust film/steel base interface (after 236 h of intermittent immersion corrosion test)

(a) 5Cr (b) 5Cr-0.3Cu-0.3Ni

Photo 2 TEM micrographs of rust particles comprising rust film (after 236 h of intermittent immersion corrosion test)

coarse, needlelike particles more significantly inhibited than the 5Cr steel. This tendency was similarly recognized for the 5Cr-1.5Ni steel and 5Cr-0.5Mo steel.

The EPMA observation of the rust film/steel base interface showed that chromium was uniformly concentrated in a larger amount in the rust film than in the base metal of the 5Cr steel, and that copper, nickel and molybdenum were contained, not as concentrated as chromium, in the rust film of the 5Cr steel to which copper-nickel, nickel and molybdenum additions were made, respectively. The overall evaluation results of the prototype steels as to rust stability are given in **Table 3**.

Table 3 Evaluation results of rust adhesion

	SM400B	5Cr	5Cr-0.3Cu-0.3Ni	5Cr-1.5Ni	5Cr-0.5Mo
Deposited rust weight	××	◎	◎	◎	◎
Loose rust	××	○	◎	◎	◎
Rust film uniformity	××	△	◎	◎	◎
Rust particle tightness	××	○	◎	◎	◎
Rust film elemental distribution	-	Cr concentrated	Cr,Cu,Ni concentrated	Cr,Ni concentrated	Cr,Mo concentrated

Poor←××<×<△<○<◎→Good

From the above results, it was presumed that the addition of 5% chromium retarded the corrosion rate and lowered the amount of rust formation and that the addition of copper and nickel, nickel, and molybdenum in combination with chromium, respectively, dissolves copper, nickel, and molybdenum together with iron and chromium in rust, inhibits the coarsening and crystallization of individual rust particles in the rust particle growth process, improves the adhesion and uniformity of rust, and reduces the amount of peeled rust.

2.4 Determination of basic chemical composition

According to the results of investigation into the effect of chromium on corrosion resistance, the basic chromium content was put at 5%. Also considering economy, the chemical composition of 5% chromium, 0.3% copper, and 0.3% nickel was selected as the optimum system for the new corrosion-resistant steel with still higher corrosion resistance and improved rust adhesion for the stacks of LNG-fired power plants.

3. Properties of WELACC5

3.1 Mill trial

The new corrosion-resistant steel of the basic 5Cr-0.3Cu-0.3Ni composition was trial produced at the mill. **Table 4** lists the chemical composition of the trial steel. In the mill trial work, 4.5-, 12-, 21-, and 30-mm thick plates were produced by the process of BOF steelmaking, secondary refining, casting, slab conditioning, reheating, plate rolling, and heat treatment. These plates were then evaluated for various service performance properties as described below.

3.2 Properties of base metal

The tensile test results of base metal are listed in **Table 5**. The respective plates exhibit strength, ductility, and bendability satisfactory for a welded structural steel of the 400 MPa class. Their Charpy impact test values are especially good.

3.3 Formability and cuttability

Simulating the fabrication of a stack, 12-mm thick plates were edge bent on a 3,000-ton press (bending load of 150 tons, 9 bends) and body bent with bending rollers (bending displacement of 10 to 20 mm, 10 bends). The bending radius and straightness were good in each test. The bending accuracy and total bending time of WELACC5 were satisfactory and comparable to those of carbon steel and stainless steel-clad carbon steel.

Table 4 Chemical composition of mill trial WELACC5 (mass%)

		C	Si	Mn	P	S	Cu	Ni	Cr	T-Al
Specification	Minimum	-	-	0.30	-	-	0.15	0.15	4.00	-
	Maximum	0.09	0.50	0.60	0.030	0.030	0.50	0.50	6.00	-
Ladle analysis		0.03	020	0.50	0.006	0.004	0.28	0.34	4.89	0.033

Table 5 Tensile test results of base metal of WELACC5

Plate thickness (mm)	Type of test specimen	Number of test specimens	Test direction	0.1% offset yield strength (MPa)	Yield point or 0.2% offset yield strength (MPa)	Tensile strength (MPa)	Elongation (%)
4.5	JIS No. 5	3	Transverse	330	336	478	37
				328	337	480	37
				328	340	482	38
12	JIS No. 1A	3	Transverse	307	311	463	28
				310	311	463	29
				311	315	464	26
21	JIS No. 1A	3	Transverse	285	297	475	29
				294	303	478	26
				297	325	484	23
30	JIS No. 1A	3	Transverse	247	262	459	32
				248	268	462	32
				249	268	461	32

Table 6 Cutting test results of WELACC5

Cutting process	Cutting shape	Cutting speed (mm/min)	Cut edge surface roughness (notched or not)
Plasma cutting	Straight	1,100	○
	Straight	1,400	○
	Straight	1,500	○
	Straight	1,600	○
	Straight	1,700	△
Gas cutting	Bevel (30°C)	280	○

WELACC5 was tested for cuttability by plasma cutting and gas cutting. The test conditions and results are given in **Table 6**. When WELACC5 was plasma cut straight at a current of 120 mA and speed of 1,600 mm/min, it was confirmed to have good plasma cuttability. It was also found to be gas cut with good results.

3.4 Weldability

3.4.1 Selection of welding materials

Welding materials for the plate thickness range of 4.5 to 30 mm were studied to meet the conditions that the weld strength should be equivalent to that of the SM400A steel and that cold cracking should not occur when the weldment was not preheated and postheated. The austenitic stainless steel SUS309 was selected as a result.

Welding of WELACC5 with austenitic welding materials is dissimilar metal welding and is feared to suffer from hot cracking of weld metal and from martensite-induced embrittlement and cracking. These problems were investigated, mainly using the Schaeffler constitution diagram, according to the compositions of WELACC5 and the welding materials. As a result, it was found that since the dilution ratio was less than 30% for shielded meal arc welding (SMAW) and flux cored arc welding (FCAW), martensite did not form, eliminating the fear of cold cracking. It was also made clear that the formation of a few percent δ-ferrite prevented hot cracking.

3.4.2 Weld cracking susceptibility

The results of tests conducted to determine the y-groove weld cracking susceptibility of WELACC5 by using 30-mm thick plates are given in **Table 7**. When WELACC5 was welded without preheat by using an austenitic filler metal, it did not crack and demonstrated satisfactory weldability.

Table 7 y-groove weld cracking susceptibility of WELACC5

(a) y-groove weld cracking test conditions

Plate thickness (mm)	Welding process	Welding material	Welding condition			
			Current (A)	Voltage (V)	Speed (cm/min)	Heat input (kJ/cm)
30	SMAW	S-309MR 4mm ϕ	170	24	15	16

(b) y-groove weld cracking test results (number of tests: 2)

Preheat temperature (°C)	Crack ratio (%)					
	Surface		Section		Root	
25	0	0	0	0	0	0
50	0	0	0	0	0	0
100	0	0	0	0	0	0

Table 8 Welding conditions of WELACC5

Welding process	Welding material	Current (A)	Voltage (V)	Speed (cm/min)	Heat input (kJ/cm)	Number of layers	Shielding gas	Interlayer temperature (K)
SMAW	309 type 3.2mm ϕ	100	24	200	7.2	15	-	≦423
FCAW	309 type 1.2mm ϕ	220	28	300	12.3	6	80%Ar +20%CO_2	≦423

SMAW: Shielded metal arc welding
FCAW: Flux cored arc welding

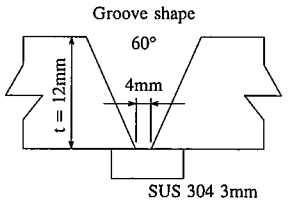

Table 9 Tensile test results of weld joints of WELACC5

Plate thickness	Welding process	Type of test specimen	Number of test specimens	Tensile strength (MPa)	Fracture position
12mm	SMAW	JIS No.1 GL = 30	2	499 494	Base metal
		JIS No.1A GL = 68	2	480 484	Base metal
	FCAW	JIS No.1 GL = 30	2	508 503	Base metal
		JIS No.1A GL = 68	2	483 485	Base metal

3.4.3 Joint properties

WELACC5 plates, measuring 12 mm in thickness, were welded under the conditions given in **Table 8** and were tensile, impact, guide bend and macroetch tested. The tensile, impact, and guide bend test results of the welded joints are shown in **Table 9**, **Fig. 9**, and **Table 10**, respectively. These test results confirmed that the tensile, impact, and guide bend properties of the WELACC5 weld joints are good and are comparable to those of weld joints of the SM400B steel. The WELACC5 plates were also welded in the vertical and horizontal positions by simulating the actual stack fabrication process, and the weld joints obtained were evaluated for properties. The weld joints had a tensile strength of 503 to 508 MPa

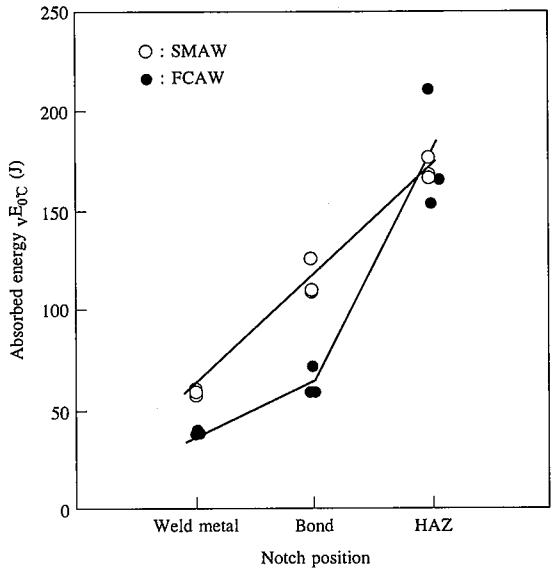

Fig. 9 Impact test results of weld joints of WELACC5

Table 10 Guide bend test results of weld joints of WELACC5

Plate thickness (mm)	Welding process	Specimen type Test method	Number of test specimens	Test results	
				Face bend	Root bend
12	SMAW	JIS A 3122 w=40 t=10 r=2t	2	Good	Good
	CO_2		2	Good	Good

and failed in the base metal, and exhibited no defects when bent over the radius of twice their thickness to an angle of 180°.

As discussed above, the weld joints of WELACC5 were confirmed to have tensile, toughness, and bend properties equal or superior to those of SM400B weld joints.

4. Stack Exposure Test Results

The exposure test results of the new corrosion-resistant steel WELACC5 in the stack duct of a LNG-fired power plant are shown in **Fig. 10**. The corrosion rate of the 5Cr-0.3Cu-0.3Ni steel is 0.0007 mm/y and is about one-third of the SM400B steel. This confirmed that WELACC5 exhibits excellent corrosion resistance in the actual stack environment. A brown corrosion product was

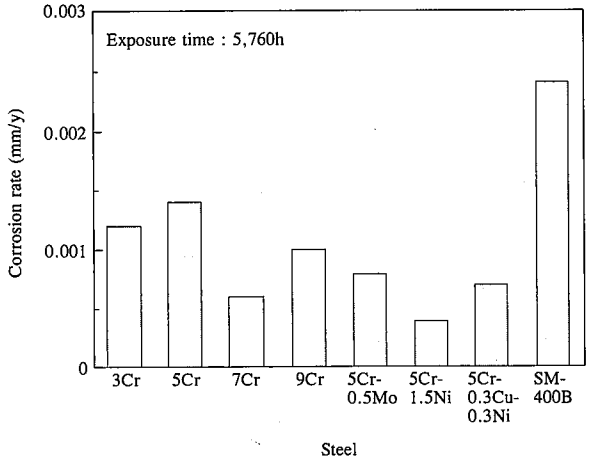

Fig. 10 Exposure test results of WELACC5 in stack environment of LNG-fired power plant

formed in a very small amount on the surface of the WELACC5 test specimens. When the corrosion product was analyzed by the X-ray diffraction technique, $(NH_4)_3H(SO_3)_2$ and $(NH_4)_2SO_4$ were identified. These compounds are deposits and found in the deposits on the stack of the LNG-fired power plant. When the surface of the WELACC5 test specimens was examined under an optical microscope with a Normarski prism, slight corrosion traces were observed. Coupled with the fact that the X-ray diffraction technique failed to detect iron rust components like iron oxide hydroxide, this suggests that WELACC5 was still in the very early stage of corrosion. The rust adhesion of WELACC5 will have to be verified by an exposure test over a longer period of time.

Weld joint specimens are now undergoing exposure test at the same site. When specimens after 8,640 h of exposure were examined, it was confirmed that localized corrosion was not caused in their weld metal, heat-affected zone, and base metal.

5. Specifications of WELACC5

Table 11 shows the main specifications of WELACC5™. WELACC5 is a low-alloy plate steel of the basic 5Cr-0.3Cu-0.3Ni composition. Chromium is added to improve its corrosion resistance, and copper and nickel are added to improve its corrosion resistance and rust scatter resistance. WELACC5 is produced in the plate thickness range of 4.5 to 30 mm and with mechanical properties, formability, and fabricability comparable to those of the SM400B steel.

Table 11 Main specifications of WELACC5™

Material	Chemical composition (mass%)								Mechanical properties			
	C	Si	Mn	P	S	Cu	Ni	Cr	0.2% offset yield strength (MPa)	Tensile strength (MPa)	Elongation (%)	Charpy absorbed energy at 273K (J)
SLACC5	0.03	0.20	0.50	0.006	0.004	0.28	0.34	5.00	311	463	28	Rolling direction : 245 Transverse direction : 206
Specified value	≦0.09	≦0.50	0.30/0.60	≦0.030	≦0.0030	0.15/0.50	0.15/0.50	4.00/6.00	245≦*	400-510*	18≦*	27≦*

*SM400B steel (plate thickness of 12 mm), specified in JIS G 3106, Rolled Steels for Welded Structures.

6. Conclusions

A new corrosion-resistant plate steel (trademarked WELACC5) was developed to ensure the maintenance-free operation of LNG-fired power plant stacks over a long period of time. WELACC5 has 5% chromium added to improve its corrosion resistance in the stack environment, has trace copper and nickel added in combination to enhance its corrosion resistance further and improve its rust adhesion (rust scatter resistance), and has its chemical composition and production process adjusted to obtain mechanical properties and weldability equivalent to those of the SM400B steel.

The results of laboratory corrosion tests and exposure tests in the stack environment of an actual LNG-fired power plant show that WELACC5 has a small corrosion rate of 0.0007 mm/y and good corrosion resistance and rust scatter resistance. Its mechanical properties are comparable to those of the SM400B steel. The use of austenitic welding materials allows WELACC5 to be welded without preheat. The WELACC5 weld joints are practically satisfactory in all respects of weldability, cracking resistance, weld joint performance, and corrosion resistance.

WELACC5 was produced by the process of BOF steelmaking and plate rolling, and the WELACC5 plates thus produced were evaluated as to various properties important for the fabrication of stacks. The evaluation results confirmed that WELACC5 had satisfactory service performance properties.

In 1997, more than 2,000 tons of WELACC5 was produced for the stacks of LNG-fired combined cycle power plants. WELACC5 is expected to find increasing usage in the stacks and ducts of LNG-fired power plants.

References

1) Abe, N.: Thermal and Nuclear Power. 46, 600 (1995)
2) Teramae, A. et al.: Fuji Seitetsu Giho. (17), 103 (1968)
3) Ebara, R. et al.: Mitsubishi Juko Giho. 27, 431 (1990)
4) Usami, A. et al.: Proceedings of 42nd Japan Corrosion Conference. 1995, p. 257